


RESEARCH

Open Access



Rab11a-dependent recycling of Glut3 inhibits seizure-induced neuronal disulfidptosis by alleviating glucose deficiency

Sijun Li^{1†}, Junrui He^{1†}, Huimin Kuang², Xiaojuan Wang¹, Muhua Zhou¹, Dongmei Li¹, Baoren Kang¹, Honghu He¹, Lina He¹, Wei Lin^{1*} and Yuan Lv^{2*} 

Abstract

Seizures can trigger neuronal glucose deficiency, thereby inducing disulfidptosis. Disulfidptosis is a novel cell death mechanism characterized by the abnormal accumulation of disulfide caused by glucose deficiency. However, the mechanism underlying disulfidptosis caused by glucose deficiency in seizures remains elusive. Rab11a-dependent recycling of glucose transporter 3 (Glut3) is closely related to glucose metabolism in neurons, which may contribute to neuronal disulfidptosis after seizures by abnormal glucose metabolism. So here we introduced a well-established in vitro model of seizures to evaluate cell survival, glucose levels, disulfidptosis biomarkers, Glut3 and Rab11a expression, the recycling ratio of Glut3, and the protein complex of Glut3-Rab11a. Cell survival rates and glucose levels were lower in the in vitro model of seizures, accompanied by elevated levels of disulfidptosis markers. Moreover, the surface expression and the recycling ratio of Glut3, as well as the protein complex of Glut3-Rab11a, were positively correlated with Rab11a expression. Lastly, Rab11 overexpression improved cell survival rates, increased glucose levels, and decreased the levels of disulfidptosis biomarkers in the in vitro model of seizure. Rab11a-dependent recycling of Glut3 inhibited seizure-induced neuronal disulfidptosis by alleviating glucose deficiency.

[†]Sijun Li and Junrui He contributed equally to this work.

*Correspondence:

Wei Lin

linweidr@hotmail.com

Yuan Lv

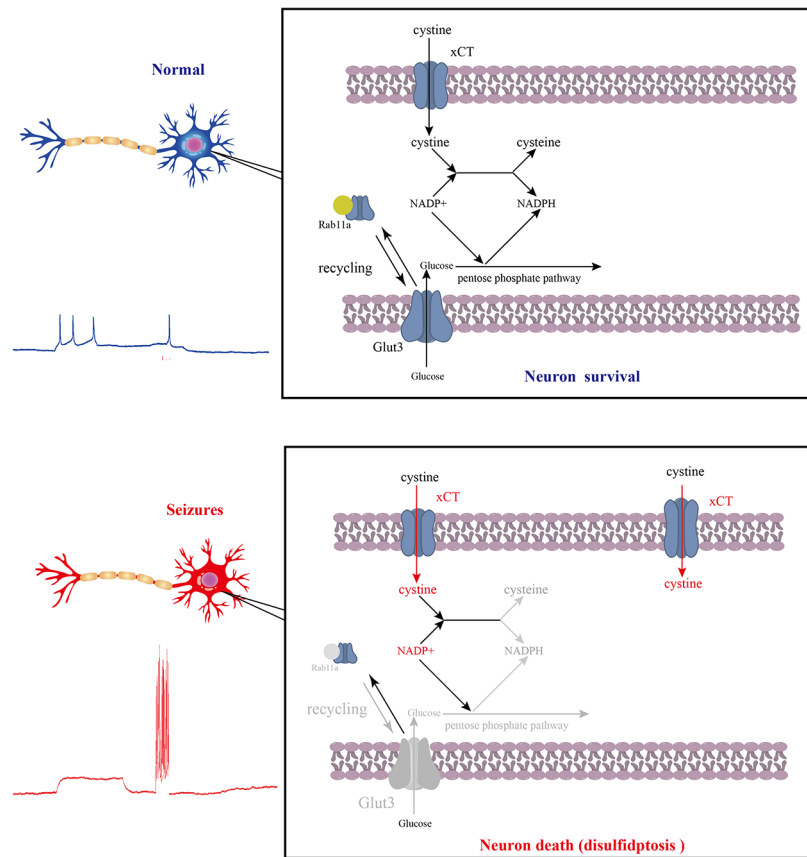
medicinepro_l@163.com

Full list of author information is available at the end of the article



© The Author(s) 2025. **Open Access** This article is licensed under a Creative Commons Attribution 4.0 International License, which permits use, sharing, adaptation, distribution and reproduction in any medium or format, as long as you give appropriate credit to the original author(s) and the source, provide a link to the Creative Commons licence, and indicate if changes were made. The images or other third party material in this article are included in the article's Creative Commons licence, unless indicated otherwise in a credit line to the material. If material is not included in the article's Creative Commons licence and your intended use is not permitted by statutory regulation or exceeds the permitted use, you will need to obtain permission directly from the copyright holder. To view a copy of this licence, visit <http://creativecommons.org/licenses/by/4.0/>. The Creative Commons Public Domain Dedication waiver (<http://creativecommons.org/publicdomain/zero/1.0/>) applies to the data made available in this article, unless otherwise stated in a credit line to the data.

Graphical Abstract



Keywords Seizures, Neurons, Glucose, Recycling, Disulfidptosis

Introduction

As is well documented, epilepsy (EP) is a complex disease caused by the synchronous discharge of neurons, with seizures as the primary manifestation [1]. Seizures are predominantly triggered by increased excitatory function and/or decreased inhibitory function of neurons, a mechanism also referred to as excitatory/inhibitory imbalance (E/I imbalance) [2–4]. However, E/I imbalance is not the only potential mechanism for seizures. Previous studies demonstrated that glucose metabolism disorders in the brain may also be involved in the occurrence and progression of seizures [5–8]. Hildebrand et al. described that lower glucose levels in the brain may be a key cause of seizures [9]. Longer durations of seizures are linked to lower glucose metabolism in the hippocampus on the ipsilateral side of the epileptic focus [10]. Moreover, low glucose metabolism in the brain may be linked to Sudden Unexpected Death in Epilepsy (SUDEP) [11]. Taken together, these studies suggest that seizures are associated with reduced glucose levels in neurons, which is likely to trigger disulfidptosis.

Disulfidptosis is considered a novel cell death mechanism characterized by the abnormal accumulation of cystine (Cyss), a type of disulfide with high intracellular cytotoxicity, that eventually results in cell death induced by disulfide stress [12]. Under physiological conditions, glucose generates a reduced form of nicotinamide adenine dinucleotide phosphate (NADPH) via the pentose phosphate pathway, which provides the reducing power to counteract the toxic effects of disulfide stress on cells. Under glucose-deficient conditions, the excessive Cyss uptake and Cyss reduction to cysteine (Cys) deplete the NADPH pool, leading to an imbalance in the NADP⁺/NADPH ratio, the accumulation of disulfides, and eventually rapid cell death [13–16]. During this process, members of the solute carrier family, SLC7A11 and SLC3A2, form complexes that facilitate cystine transport and accumulation into cells [17]. Even worse, these complexes promote abnormal disulfide bonding in cytoskeletal proteins such as actin, resulting in F-actin collapse [16, 18, 19]. Notably, glucose is the primary source of energy for the brain [20]. Previous studies suggested that

reduced glucose levels in the brain are associated with neurological disorders [21, 22], with disulfidptosis playing a central role in the pathogenesis of these diseases [23, 24].

Increasing extracellular glucose levels does not inhibit seizures but rather increases the discharge frequency [25], potentially exacerbating cellular damage [26]. Indeed, exogenous glucose supplementation cannot address seizure-induced cell death, which may be related to glucose uptake mechanisms in neurons. Glucose transporter 3 (Glut3) on the neuronal surface can uptake glucose into cells and provide raw materials for energy metabolism [27, 28]. Down-regulating Glut3 expression impairs Glut3 transport, resulting in dysregulated glucose uptake by neurons and glucose deficiency-induced cell death [29, 30]. The transport of Glut3 from the cell to the membrane, i.e., Glut3 recycling, is dependent on the Rab11 pathway [29]. Rab11 is a marker for endosomal recirculation that regulates vesicle trafficking from the endosomal compartments and early endosomes to the trans-Golgi network and plasma membrane [31]. Rab11 mediates membrane-related transport processes, such as exocytosis and recirculation of membrane proteins to the plasma membrane [32]. Rab11 has multiple members, among which Rab11a is ubiquitous in multiple organs. Abnormal Rab11a function has been associated with seizures [33]. Nevertheless, the effect of Rab11a-mediated Glut3 recycling on seizure-induced neuronal disulfidptosis remains underexplored. Therefore, an in vitro model of seizure was constructed in the present study to evaluate the potential link between Glut3, disulfidptosis mechanisms and seizures by assessing cell survival, glucose levels, disulfidptosis biomarkers, Glut3 and Rab11a expression, and Glut3 recycling.

Materials and methods

Construction of the in vitro model of seizure

Neurons were harvested from newborn Sprague Dawley (SD) rats (24 h-old) purchased from the Animal Center of Guangxi Medical University. Primary neurons were cultured based on the methods outlined in a previous study [4]. The conditions for cell culture are as follows: 5% CO₂ and 37 °C. Two types of medium, serum-neurobasal medium and serum-free-neurobasal medium were used. The serum-neurobasal medium was used for the first 10 h of in vitro culture. After 10 h, the serum-neurobasal medium was removed and replaced with a serum-free neurobasal medium. The serum-neurobasal medium was as follows: 88% GibcoDulbecco's Modified Eagle Medium: F-12(DMEM/ F12)(Gibco, A4192001), 1% Glutamax (Gibco, 35050061), 1% penicillin–streptomycin (Gibco, 15140–122) and 10% serum (Gibco, A3160902). The serum-neurobasal medium was as follows: 96%

Neurobasal™-A (Gibco,10888022), 1% Glutamax (Gibco, 35050061), 1% penicillin–streptomycin (Gibco, 15,140–122) and 2% B27 supplement (Gibco, 17504044). On Day in vitro 15 (DIV-15), neurons were divided into a control (Ctrl) group and a magnesium-free (Mg²⁺-free) group and subsequently exposed to two different extracellular fluids (5% CO₂, 37 °C, 3 h). Specifically, neurons in the Ctrl group were exposed to normal extracellular fluid, and those in the Mg²⁺-free group were exposed to Mg²⁺-free extracellular fluid. The proportion of extracellular fluid was as follows: 145 mM sodium chloride (NaCl), 2.5 mM potassium chloride (KCl), 10mM HEPES, 2mM calcium chloride (CaCl₂), 10mM glucose, 0.002mM glycine, and 1mM magnesium chloride (MgCl₂). The proportion of Mg²⁺-free extracellular fluid was as follows: 145mM NaCl, 2.5mM KCl, 10mM HEPES, 2mM CaCl₂, 10mM glucose, 0.002mM glycine.

Lentivirus (LV) was purchased from Sangon Biotechnology (Shanghai) Co., Ltd., including the LV negative control (NC) group (titer: 1 × 10⁹ TU/mL) and LV over-expressing Rab11a (OE) group (titer: 2 × 10⁸ TU/mL). To explore optimal multiplicity of infection (MOI), neurons in DIV-3 were exposed to LV with different MOI (MOI=0, 1, 5, 10, 50, 100). After 24 h of exposure, the serum-free neurobasal medium containing the LV was replaced back into the normal serum-free neurobasal medium. On DIV-15, the neurons were used to measure cell survival and protein expression. After preliminary exploration, the best value of MOI was determined. Based on best value of MOI, neurons (DIV-3) were transfected with LV. On DIV-15, LV-transfected neurons were exposed to Mg²⁺-free extracellular fluid.

The extracellular fluid, Mg²⁺-free extracellular fluid for the in vitro model, extracellular fluid, and intracellular fluid for action potential (AP) detection were prepared according to the methods established in our previous study [4]. The proportion of extracellular fluid (pH=7.4) for AP detection was as follows: 122 mM NaCl, 2 mM KCl, 25mM HEPES, 2mM CaCl₂, 4mM MgCl₂, and 10mM glucose,. The proportion of intracellular fluid (pH=7.3) for AP detection was as follows:110 mM KCl, 1mM NaCl, 2mM ethylene glycol tetraacetic acid (EGTA), 25mM HEPES, 4 mM adenosine 5'-triphosphate magnesium salt (Mg-ATP), 0.3 guanosine 5'-(disodium dihydrogen triphosphate) (Na₂-GTP) and 10mM phosphocreatine. The resistance of patch electrodes was 3–6 MΩ. Digidata 1550 B patch-clamp amplifier and Axon Digidata 1550 B 16-bit data acquisition system were employed to obtain the APs (clamping voltage, -70 mV; mode, whole-cell recording). The pClamp 10.7 data acquisition software were utilized to analyze the data of APs.

Glucose level measurement and cystine uptake assays

After lysis, glucose levels were determined in neurons using a glucose content assay kit (BC2500, Solarbio) [34, 35]. A Cystine Uptake Assay Kit was utilized to perform the cystine uptake assays. The Infinite m200 PRO (TECAN) was employed to measure glucose levels and cystine uptake.

Analysis of neuronal survival rate

The 3-(4,5-dimethylthiazol-2-yl)-2,5-diphenyltetrazolium bromide (MTT) kit (Boster, AR1156) was used to measure cell survival rates. The Infinite m200 PRO (TECAN) was employed to measure MTT.

NADP⁺ and NADPH measurements

The NADP(H) Content Assay Kit (BC1105, Solarbio) was used to determine NADP⁺ and NADPH levels [36]. The Infinite m200 PRO (TECAN) was employed to measure NADP⁺ and NADPH levels. Finally, the ratio of NADP⁺ / NADPH was calculated.

Western blot analysis

A protein extraction kit (Invent Biotechnologies, SD-001/SN-002; SM-005) was utilized to extract the total protein and surface protein of neurons. Western blot analysis was performed based on the methods described in previous studies [4, 30]. Primary antibodies used in the current study were anti- Glut3 antibody (Santa, sc-74399) (dilution: 1:500) [37], anti-xCT (xCT protein was coded by the SLC7A11 gene) antibody (Abcam, ab307601, dilution: 1:500), anti-Rab11A antibody (Abcam, ab128913, dilution: 1:500) anti-GAPDH antibody (Sangon Biotech, D110016) (dilution: 1:10000), anti-alpha Tubulin1 antibody (abcam, ab7291, dilution: 1:10000) and anti-ATP1A1 antibody (Proteintech, 14418-1-AP) (dilution: 1:10000). The secondary antibodies were IRDye 800CW-conjugated goat anti-rabbit immunoglobulin IgG (product #5151, 1:2000, CST) and DyLightTM800-conjugated anti-mouse IgG (H+L) (product #5257, 1:5000; CST). Total proteins were normalized to internal reference proteins GAPDH or alpha Tubulin1 using Image J software. Surface proteins were normalized against ATP1A1.

Colocalization assay

Colocalization staining of neurons was conducted according to the method outlined in a previous study [4]. Neurons were incubated with the first primary antibody, anti-Glut3 antibody (Santa, sc-74399) (dilution: 1:50) overnight at 4 °C. After washing with PBS, they were incubated with a fluorescent secondary antibody (Boster, BA1101) (dilution: 1:100) (45 min, 37 °C). Neurons were marked in green fluorescent. Thereafter, neurons were incubated with a second primary antibody, anti-Rab11A antibody (Abcam, ab316152) (dilution: 1:100), overnight

at 4 °C. After washing with PBS, they were incubated with a fluorescent secondary antibody (Boster, BA1090) (dilution: 1:100) (45 min, 37 °C), with neurons marked in red fluorescent. Finally, the neurons were incubated with a DAPI staining solution for 3 min at room temperature. Fluorescence images of neurons were captured using a microscope (Olympus BX53).

Co-immunoprecipitation (Co-IP) assay

Total natural proteins were extracted using the protein extraction kit (Invent Biotechnologies, SD-001/SN-002) [38]. To generate the antigen-antibody complex, the natural proteins were combined with anti-Glut3-antibody (Santa, sc-74399) (overnight, 4 °C). CO-IP analysis was performed using the immunoprecipitation kit (Sangon Biotech, C600689). Protein samples were separated via SDS-PAGE and transferred to the NC membrane by wet transfer cells (Bio-Rad) (Merck Millipore Ltd.). Primary antibodies for western blot analysis were as follows: anti-Glut3 antibody (Santa, sc-74399) (dilution, 1:500) [37], anti-Rab11A antibody (Abcam, ab128913; dilution, 1:500).

Recycling assay for Glut3

The neurons were incubated at room temperature for 10 min with anti-Glut3 antibody (Santa, sc-74399) (dilution: 1:50). Next, they were washed with phosphate buffer (PBS) at 37 °C to remove unbound antibodies, and the neurons were cultured in an antibody-free medium at 37 °C for 20 min to induce the internalization of antibody-binding receptors. Subsequently, antibodies retained on the neuronal surface were incubated on ice for 4 min in 0.5 M of peel buffer (0.5 M NaCl and 0.2 M acetic acid). Then, neurons were washed with frozen PBS and incubated in a normal medium at 37 °C for 90 min to promote receptor recycling. The neurons were then immobilized with 4% polyformaldehyde and blocked with 5% bovine serum albumin. Glut3 recycled to the surface was detected by incubating neurons with a red fluorescent secondary antibody (Boster, BA1031). Neurons were permeabilized using 0.25% Triton X-100, and Glut3 was detected using a green fluorescent secondary antibody (Boster, BA1126). A microscope (Olympus BX53) was utilized to observe and capture fluorescence images of neurons. A total of 9 neurons in each group were used to calculate optical density. Recycling ratio = surface fluorescence signal/(surface signals + intracellular signals).

Statistical analysis

The data are expressed as the mean ± standard deviation. Experimental data were compared between 2 groups using the independent sample *t* test. Experimental data were compared among groups (>2 groups) using one-way analysis of variance. SPSS 25.0 was used for the statistical

analysis. A p value of <0.05 was considered statistically significant.

Results

Seizures led to glucose deficiency and disulfidptosis in neurons

Neurons exposed to Mg^{2+} -free extracellular fluid for 3 h produce synchronized firing, which is considered as an in vitro model of seizures [4]. After exposed to Mg^{2+} -free extracellular fluid for 3 h, the neuronal APs were detected by patch clamp. The amplitude and frequency of neuronal APs were significantly higher in the Mg^{2+} -free group ($n=6$ in each group; vs. Ctrl, $p<0.01$; Fig. 1A), which suggested the in vitro model of seizures was successfully constructed. The morphology of the neurons was then observed. In normal neurons, the cell bodies are round and full, showing a round or oval shape, the neurites are obvious, and the neurons are connected into a clear neural network structure. The neurons in the Ctrl group was with same morphology as normal neurons, which had full cell bodies and prominent network structures. In contrast, the neurons in the Mg^{2+} -free group were with significantly lower numbers, displaying significant cell edema and disorganized neural network structures (Fig. 1B). Meanwhile, the level of neuronal glucose in the Mg^{2+} -free group was significantly lower compared to the control group ($n=6$ in each group; vs. Ctrl, $p<0.01$; Fig. 1C). Besides, the results of the MTT assay revealed significantly lower survival rates of neurons in the Mg^{2+} -free group compared to the control group ($n=6$ in each group; vs. Ctrl, $p<0.01$; Fig. 1C). To determine whether disulfidptosis is involved in seizure-induced cell death, the disulfidptosis markers were explored. In the Mg^{2+} -free group, alterations in the levels of disulfidptosis markers were noted. For instance, the expression level of α CT was significantly higher in the Mg^{2+} -free group compared to the control group ($n=6$ in each group; vs. Ctrl, $p<0.01$; Fig. 1D). Likewise, the NADP/NADPH ratio was significantly higher ($n=6$ in each group; vs. Ctrl, $p<0.01$; Fig. 1D). Lastly, the level of Cyss uptake was significantly higher ($n=6$ in each group; vs. Ctrl, $p<0.01$; Fig. 1D). Those results demonstrated that disulfidptosis may play a significant role in seizures.

Relationship between the recycling ratio of Glut3 and the expression of Rab11a

The two proteins, Glut3 and Rab11a, were involved in glucose metabolism in neurons [39, 40] and may be the key factors in disulfidptosis. To investigate the relationship between Glut3 and Rab11a in seizures, the expression of these two proteins were detected. On the one hand, the results of western blot analysis demonstrated that the total Glut3 protein levels were comparable between the Mg^{2+} -free group and the control group

($n=6$ in each group; vs. Ctrl, $p>0.05$, Fig. 2A). On the other hand, the total protein expression level of Rab11a was significantly lower in the Mg^{2+} -free group ($n=6$ in each group; vs. Ctrl, $p<0.01$, Fig. 2A). At the same time, the protein expression level of Glut3 on the neuronal surface was significantly lower in the Mg^{2+} -free group compared to the control group ($n=6$ in each group; vs. Ctrl, $p<0.01$, Fig. 2A). To further clarify the cause of reduced Glut3 on the neuronal surface, the recycling of Glut3 was analyzed. As anticipated, the recycling assay suggested that the recycling ratio of Glut3 was lower in the Mg^{2+} -free group (9 cells in each group; vs. Ctrl, $p<0.01$, Fig. 2A). To investigate the potential link between Rab11a and Glut3, neurons were transfected with LV. In this experiment, the optimal value of MOI needs to be determined. Firstly, the effects of different MOI values of LV on the survival rate of neurons were examined. With MOI greater than 10, the survival rate of neurons was significantly reduced, even less than 50% ($n=6$ in each group; vs. MOI = 0, $p<0.01$, Fig. 2C). Since high concentrations of LV (MOI = 50, MOI = 100) can lead to excessive neuronal mortality, these two groups of LV-transfected neurons were excluded. Subsequently, the transfected neurons were measured for Rab11a expression to determine the optimal MOI value. The expression of Rab11a was most significantly increased in MOI = 5 group and MOI = 10 group ($n=6$ in each group; vs. MOI = 0, $p<0.05$, Fig. 2D). Since the survival rate of neurons in the MOI = 5 group was significantly higher than that of neurons in the MOI = 10 group, MOI = 5 was the optimal MOI value. After transfection with LV (MOI = 5), neurons in both the NC group and OE group were exposed to Mg^{2+} -free conditions. The total protein expression level of Glut3 was similar between the OE and NC groups ($n=6$ in each group; vs. NC, $p>0.05$, Fig. 2E). Conversely, the total protein expression level of Rab11a was higher in the OE group ($n=6$ in each group, vs. NC, $p<0.01$, Fig. 2E). Similarly, the protein expression level of Glut3 on the neuronal surface was higher in the OE group compared to the NC group ($n=6$ in each group, vs. NC, $p<0.01$, Fig. 2E). Overall, the recycling assay indicated that the recycling ratio of Glut3 was higher in the OE group (9 cells in each group vs. Ctrl, $p<0.01$, Fig. 2F).

Interaction between Glut3 and Rab11a

To investigate the relationship between Glut3 and Rab11a, colocalization analyses were performed. The results showed that Glut3 and Rab11a were both expressed on neurons (Fig. 3A), signaling a colocalization relationship between both proteins. The CO-IP assay indicated that the number of Glut3-Rab11a protein complex was significantly lower in the Mg^{2+} -free group compared to the control group ($n=6$ in each group; vs. Ctrl, $p<0.01$, Fig. 3B), whereas the number of Glut3-Rab11a

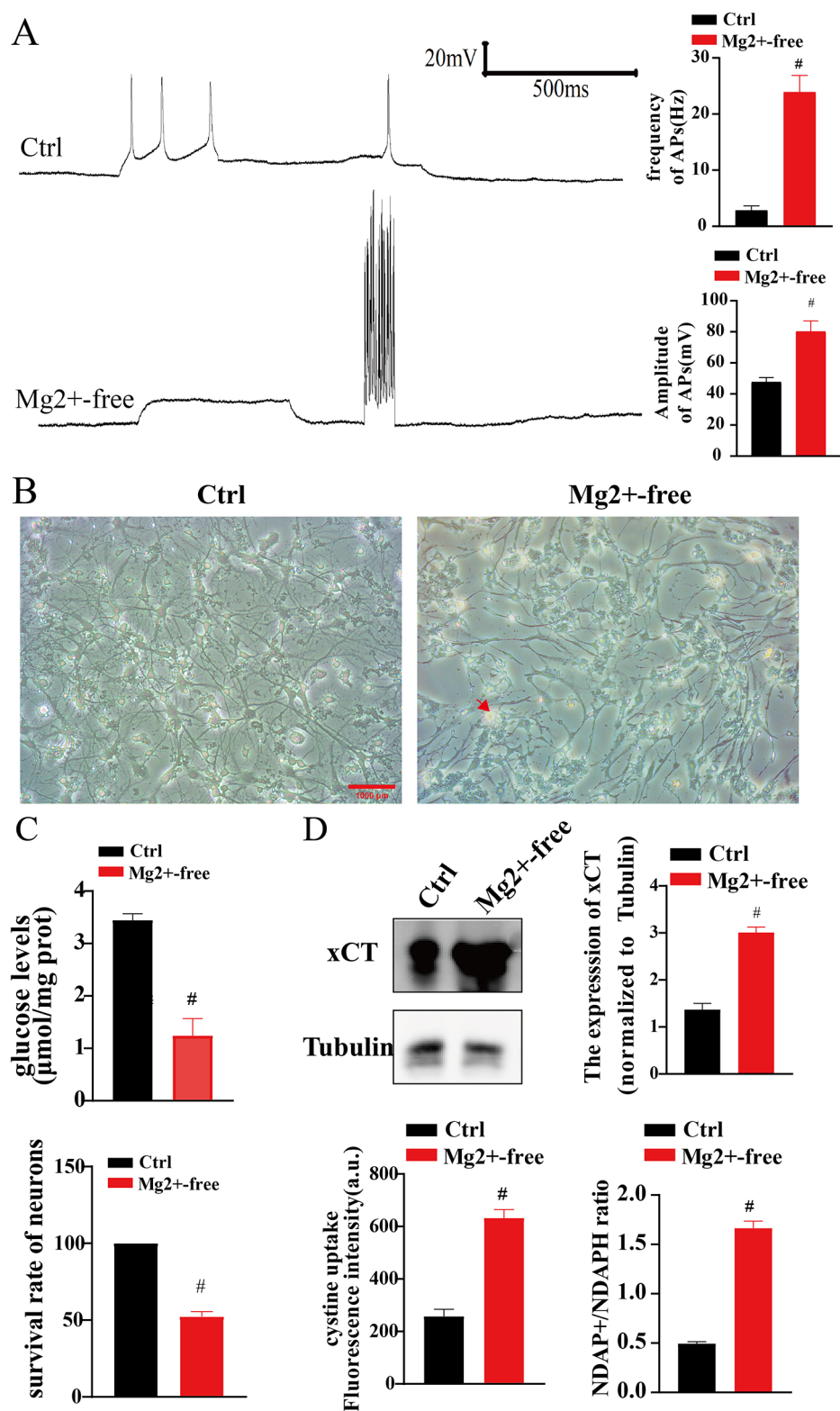


Fig. 1 Seizures can lead to glucose deficiency and disulfidptosis in neurons. **A** The amplitude and frequency of neuronal APs were significantly higher in the Mg2+-free group (6 cells in each group;#, $p < 0.01$). **B** Neurons in the Ctrl group (x200): Neuronal bodies were full, with visible axons. Neurons in the Mg2+-free group were swollen and ruptured. Additionally, the number of neurons was significantly lower, with significant cell edema and level and no visible neural network structure. Red arrows indicate swollen and ruptured neurons. Scale: 100µm. **C** Neuronal glucose levels were significantly lower in the Mg2+-free group. The survival rate of neurons in the Mg2+-free group was significantly lower ($n = 6$ in each group; * $p < 0.05$; # $p < 0.01$). **D** xCT expression, the NADP/NADPH ratio, and the level of Cys uptake were significantly increased ($n = 6$ in each group; # $p < 0.01$).

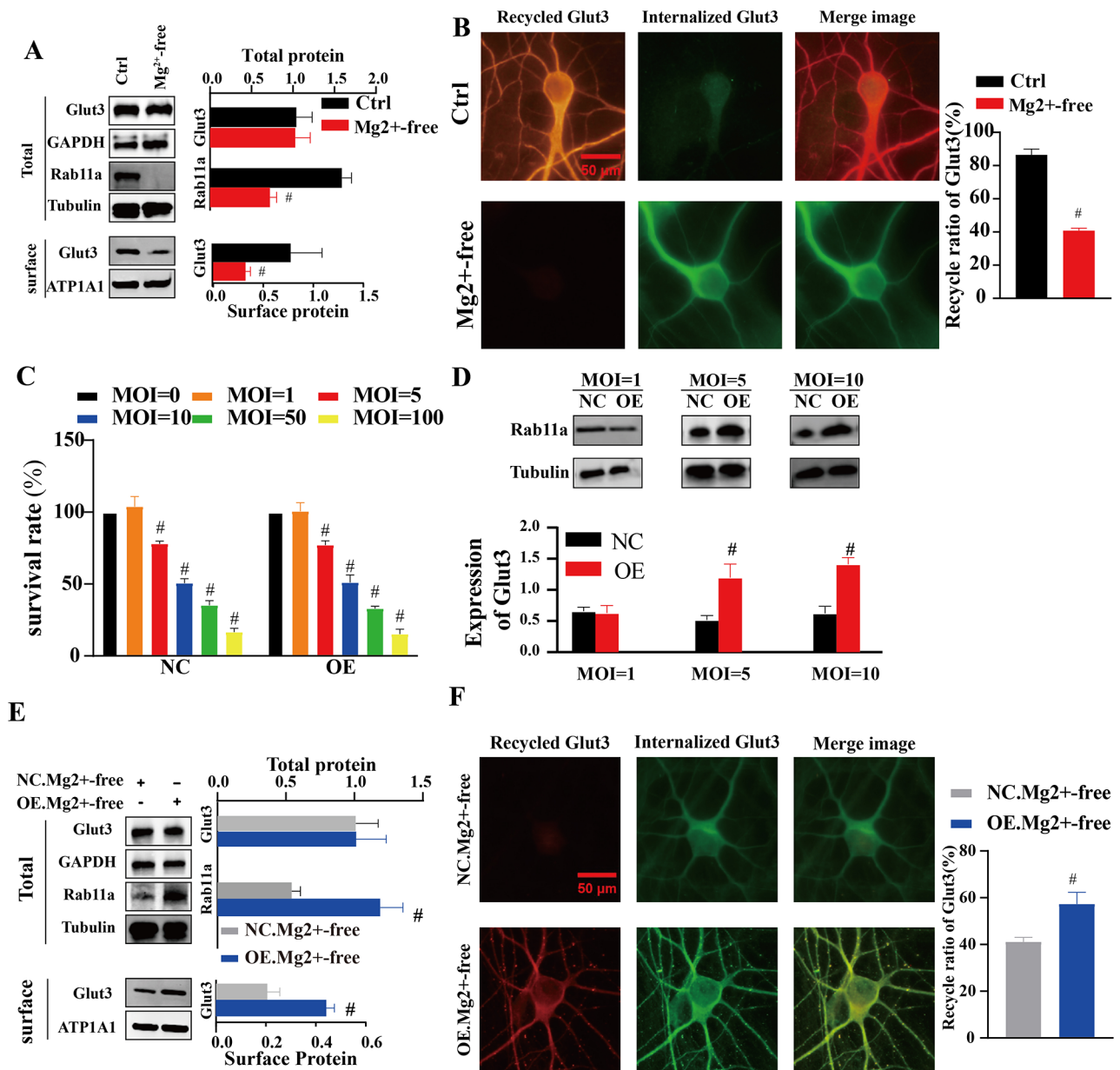


Fig. 2 Relationship between the recycling ratio of Glut3 and Rab11a expression. **A** Total protein levels of Rab11a were lower in the Mg²⁺-free group. Surface Glut3 protein expression levels on neurons were lower in the Mg²⁺-free group ($n=6$ in each group; $p<0.01$). **B** The recycling ratio of Glut3 was lower in Mg²⁺-free group (9 cells in each group; $p<0.01$) ($\times 600$, Scale: 50 μ m). **C** The survival rate of neurons in different value of MOI between of NC group and OE group. The survival rate of neurons in NC group ($n=6$ in each group; #, vs MOI=0, $p<0.01$). The survival rate of neurons in OE group ($n=6$ in each group; #, vs MOI=0, $p<0.01$). **D** The total protein expression level of Rab11 in different value of MOI between of NC group and OE group. In MOI=5 and MOI=10, the total protein expression level of Rab11a was higher in the OE group ($n=6$ in each group; $p<0.01$). **E** The total protein expression level of Rab11a was higher in the OE group. Surface Glut3 protein expression levels on neurons were higher in the OE group ($n=6$ in each group; # $p<0.01$). **F** The recycling ratio of Glut3 was higher in the OE group (9 cells in each group; # $p<0.01$) ($\times 600$, Scale: 50 μ m).

protein complex was higher in the OE group ($n=6$ in each group; vs. NC, $p<0.01$, Fig. 3C).

Rab11 alleviated glucose deficiency and inhibited seizure-induced neuronal disulfidptosis

To clarify whether Rab11a could inhibit seizure-induced neuronal disulfidptosis and protect neurons, neuronal

survival and disulfidptosis markers were again explored. After exposure to a Mg²⁺-free medium for 3 h, neuronal synchronous discharges were observed in both the NC and OE groups. Nevertheless, differences in the amplitude and frequency of APs between the NC group and the OE group were non-significant ($n=6$ in each group; vs. NC, $p>0.05$, Fig. 4A). In the NC group, there were fewer neurons with

round or oval bodies and obvious neurites. These neurons were observed with significant cell edema and the disorder of neural network structures. On the contrary, there were lots of neurons with round or oval bodies and obvious neurites in OE group. These neurons were observed with full bodies and obvious network structures (Fig. 4B). Moreover, the glucose level of neurons was significantly higher in the OE group compared to the NC group ($n=6$ in each group; vs. NC, $p<0.01$, Fig. 4C). In addition, the results of the MTT assay showed that the survival rate of neurons was significantly higher in the OE group compared to the NC group ($n=6$ in each group; vs. NC, $p<0.05$, Fig. 4C). Compared with the NC group, the expression level of xCT was significantly lower in the OE group compared to the NC group ($n=6$ in each group; vs. NC, $p<0.01$, Fig. 4D). The NADP/NADPH ratio was significantly higher in the OE group ($n=6$ in each group; vs. NC, $p<0.01$, Fig. 4C), whereas the level of cystine uptake was significantly lower ($n=6$ in each group; vs. NC, $p<0.01$, Fig. 4C).

Discussion

Seizures could lead to various serious consequences, including neuronal death, neuronal injury, and alteration of neuronal networks [41]. These consequences appear to be related to lower glucose metabolism, especially glucose deficiency [30, 42]. Seizures may result in lower glucose metabolism in the hippocampus on the ipsilateral side of the epileptic focus [10]. However, increasing extracellular glucose levels does not inhibit seizures but rather increases the discharge frequency [25], potentially exacerbating cellular damage [26]. Previous studies have shown that seizures inhibit cellular glucose uptake [43, 44], thereby reducing cellular glucose levels [45], which may account for exacerbating seizures by elevated extracellular glucose levels. Therefore, elucidating the causes underlying impaired glucose uptake by neurons may assist in unraveling seizure-induced neuronal glucose deficiency. Neurons primarily uptake glucose through Glut3, which is located on the neuronal surface [46]. Glut3, encoded by the *Slc2a3* gene, contains 12 transmembrane helices comprising a regulated central hydrophilic pore and intracellular N- and C-terminal ends [47]. The low expression of Glut3 is considered as the potential pathogenesis of Alzheimer's disease [48]. However, the relationship between Glut3 and seizures is not clear. In our study, based on the in vitro model of seizures, no significant change in the expression level of Glut3 was observed in neurons, the level of Glut3 on the neuronal surface was significantly decreased. These result indicated that the reduced Glut3 on neuronal surface may be associated with the impaired glucose uptake and seizure-induced neuronal glucose deficiency. Glut3 recycling is considered as be a key factor affecting the amount of Glut3 on the neuronal surface [29]. To investigate the the

effects of seizures on Glut3 recycling, the recycling assay was performed. The result showed that the seizures could limit the Glut3 recycling. Whereas, the underlying mechanism of Glut3 recycling in seizures remains unclear.

The recycling of the neuronal Glut3 is mediated by the Rab11 [29]. Rab11a, the member of the Rab11, is ubiquitous in multiple organs [31]. Rab11a, the a recycling endosome regulator, could regulate the recycling of some proteins in neurons [49–51]. Previous studies demonstrated that the deficiency of Rab11a was the pathogenesis of Huntington's disease [29, 40]. Hamdan et al. suggested that abnormal Rab11a function has been associated with seizures [33]. We found the expression of Rab11a was decreased in seizures, suggesting the Rab11a may play a key role in the underlying mechanism associated with seizures. To further elucidate the role of Rab11a in the regulation of Glut3 in seizures, neurons were transfected with LV to up-regulate the expression of Rab11a. These neurons overexpressing Rab11a were subsequently exposed to Mg^{2+} -free fluid, and the expression of Glut3 on the surface and the recycling ratio of Glut3 were increased. These results jointly suggested that Rab11a may up-regulate Glut3 levels on neuronal surfaces by promoting Glut3 recycling. More importantly, it was shown that Rab11a can promote protein transport by binding to proteins [31]. Furthermore, colocalization and CO-IP assays displayed the interaction between Rab11a and Glut3. In the in vitro model of seizures, the number of protein complex formed by Glut3 and Rab11a was decreased, whilst the number of Glut3-Rab11a protein complexes was higher in neurons overexpressing Rab11a. Hence, we concluded that Rab11a promoted the recycling of Glut3 through binding to Glut3, and seizures could inhibit the recycling of Glut3 by down-regulating the expression of Rab11a and reducing the the number of Glut3-Rab11a protein complexes.

Glucose deficiency induced by seizures can cause neuronal death, which in turn can exacerbate seizures [26]. Neurons undergo programmed death after seizure, including necrosis, apoptosis, pyroptosis and ferroptosis [52–55]. Liu et al. found a novel cell death mechanism, disulfidptosis. Interestingly, this new type of cell death could not be inhibited by ferroptosis, apoptosis, necroptosis and autophagy inhibitors [12]. Disulfidptosis is characterized by the abnormal accumulation of Cyss (one disulfide) caused by glucose deficiency and ameliorating glucose deficiency effectively inhibits disulfidptosis [12]. Previous studies have concluded that seizures can decrease the levels of cellular glucose [45], thereby stimulating disulfidptosis [13–16]. However, the potential relationship between seizures and disulfidptosis should be investigated further. We found that the glucose level and cell survival rate of neurons were significantly decreased in the in vitro model of seizures. Then, the levels of disulfidptosis markers were measured. The results unveiled that the expression level of xCT, NADP/NADPH

ratio, and Cyss uptake level were increased, indicating that seizures led to glucose deficiency in neurons, depletion of NADPH, and an imbalance in the NADP/NADPH ratio, resulting in the inability of neurons to effectively clear Cyss. Disulfidptosis is a complex cell death mechanism that also involves mitochondrial respiratory chain complex I which also plays a vital role in NADP/NADPH metabolism [56–58]. In addition, xCT overexpression drove Cyss uptake by neurons, which may exacerbate disulfidptosis [16, 18, 19]. These factors collectively resulted in the excessive accumulation of disulfide and induced disulfidptosis, in which glucose appears to play an important role [13–16]. Maintaining glucose levels in neurons may be critical for inhibiting disulfidptosis. Interestingly, the glucose level and cell survival rate were higher in neurons overexpressing Rab11a. Besides, xCT expression, NADP/NADPH ratio, and Cyss uptake were lower. Overall, these results suggest that Rab11a can inhibit seizure-induced neuronal disulfidptosis to improve the neuronal survival rate.

Taken together, Rab11a can increase the number of Glut3-Rab11a protein complexes, thus facilitating Glut3 recycling and increasing Glut3 expression on the cell membrane. The up-regulation of Glut3 on the surface promotes neuronal glucose uptake, minimizes NADPH consumption, maintains the NADP/NADPH balance, and thus allows neurons to effectively clear Cyss. At the same

time, the expression of xCT was down-regulated, which prevented neurons from uptaking Cyss, reduced the accumulation of disulfide in cells, and finally inhibited disulfidptosis. However, overexpression of Rab11a in neurons did not inhibit synchronous discharge. Navchaa Gom-bodorj et al. suggested that Rab11a could promote cell proliferation [59]. Aberrant Rab11a-dependent trafficking of the neuronal surface protein may causes cell death [60]. Therefore, Rab11a in neurons may play the roles in improving neuronal survival and protecting neurons.

Neuronal death induced by seizures may result in cognition impairment [61], drug-resistant epilepsy [62], depression [63], etc. What’s worse, neuronal death leads to abnormal neural networks and hippocampal sclerosis, which could exacerbate the severity of epilepsy and increases the frequency of seizures [64–66]. Protecting the neurons could attenuate the severity of epilepsy and decrease the frequency of seizures [67, 68], improving the prognosis and life quality of individuals with epilepsy. Our study revealed that Rab11a may be a target for treating epilepsy and protecting neurons. Nevertheless, some limitations of this study cannot be overlooked. To begin, this study was exclusively based on an in vitro model, and the results were not validated in in vivo models. Future studies that construct animal models are warranted. Secondly, the sequence of changes in xCT expression,

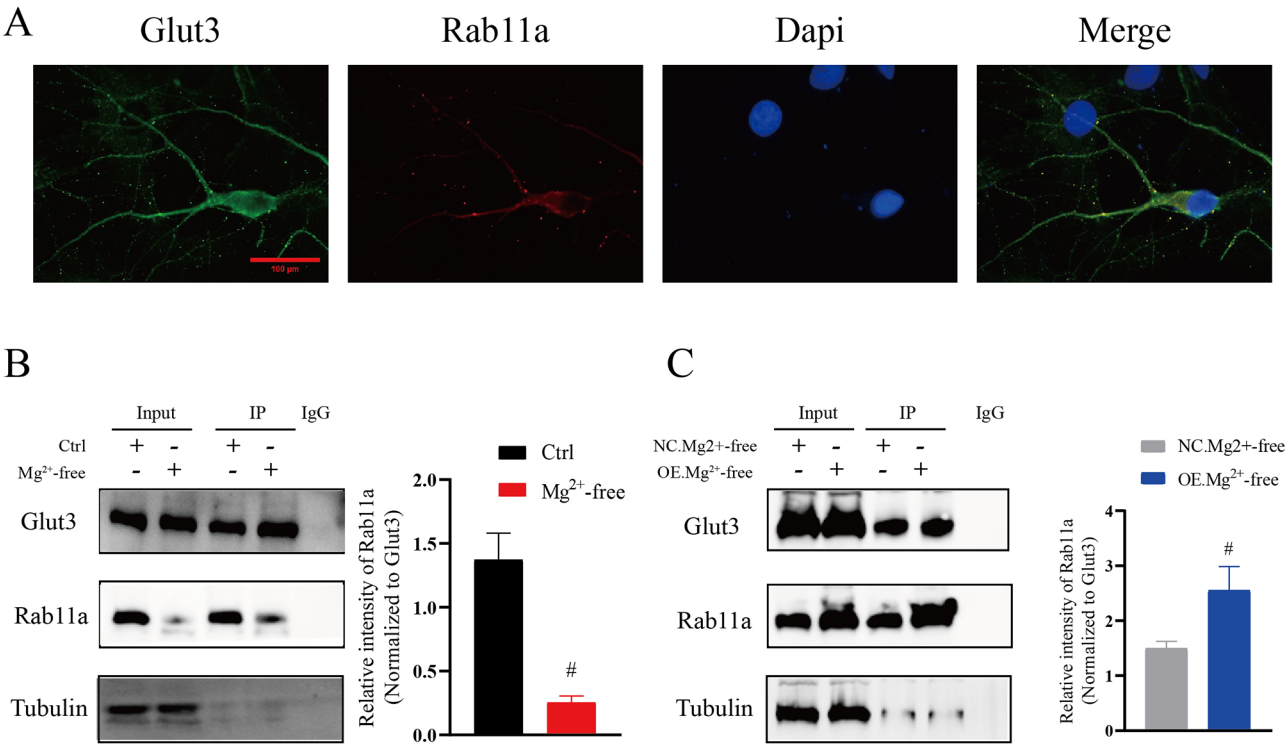


Fig. 3 Interactions between Glut3 and Rab11a. **A** Glut3 and Rab11a were both expressed on neurons (x600, Scale: 100 μm). **B** The number of Glut3-Rab11a protein complex was decreased in the Mg2+-free group (n=6 in each group; # p<0.01). **C** The number of Glut3-Rab11a protein complex was increased in the OE group (n=6 in each group;#p<0.01)

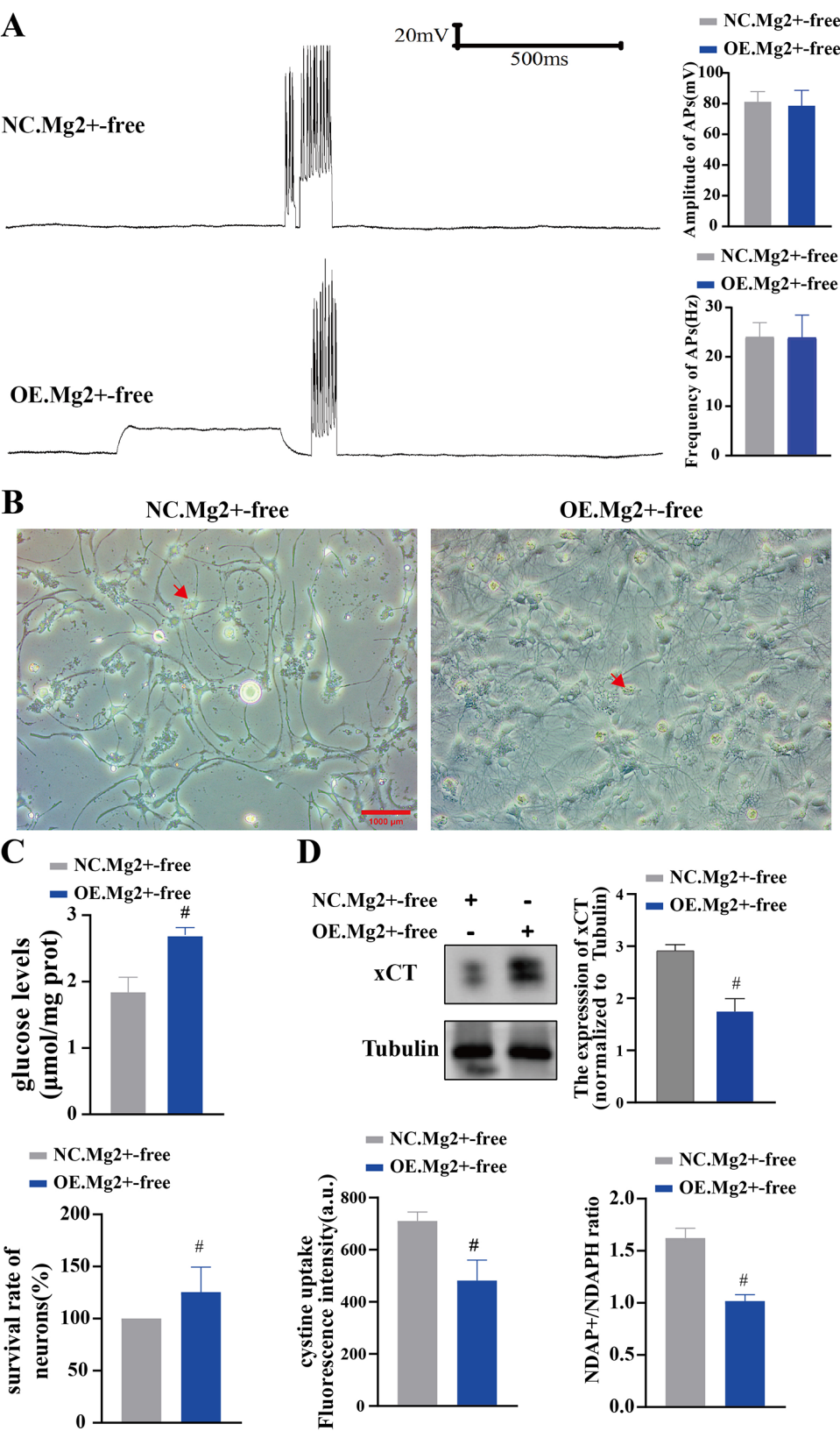


Fig. 4 (See legend on next page.)

(See figure on previous page.)

Fig. 4 Rab11 alleviated glucose deficiency and inhibited seizure-induced neuronal disulfidptosis. **A** After exposure to Mg²⁺-free for 3 h, the amplitude and frequency of APs were comparable between the NC and OE groups. **B** Neurons in the NC group (×200): the number of neurons was significantly reduced, with significant cell edema and level and no evidence of a neural network structure. Neurons in the OE group (×200): the neuronal bodies were full, with visible axons and the presence of a network structure. Red arrows represent swollen and ruptured neurons. Scale: 100 μm. **C** Neuronal glucose levels were significantly higher in the OE group, whereas the survival rate of neurons was significantly lower ($n=6$ in each group; $\#p<0.01$). **D** xCT expression, the NADP/NADPH ratio, and the level of Cys uptake were significantly decreased ($n=6$ in each group; $\#p<0.01$)

NADPH levels, and Cyss uptake during seizures were not assessed in this study. Finally, the role of the mitochondrial complex in seizure-induced disulfidptosis necessitates further research.

Conclusion

In conclusion, our results corroborated that Rab11a-dependent recycling of Glut3 inhibited seizure-induced neuronal disulfidptosis by alleviating glucose deficiency, which may be a novel target for the treatment of epilepsy and neuroprotective strategies in the future.

Supplementary Information

The online version contains supplementary material available at <https://doi.org/10.1186/s13578-025-01396-9>.

Supplementary Material 1

Acknowledgements

We thank Home for Researchers editorial team (www.home-for-researchers.com) for language editing service.

Author contributions

Sijun Li and Junrui He designed the implementation of the research, drafted the preliminary papers, performed the in vitro model and participated in the investigations. Huimin Kuang, Xiaojuan Wang and Muhua Zhou performed the western blot. Dongmei Li and Baoren Kang performed the Recycling assay. Honghu He and Lina He performed the CO-IP assay. Wei Lin and Yuan Lv were responsible for data analysis and data visualization. Yuan Lv participated in the research design and implementation, manuscript revision, and supervised the study. All the authors read and approved the final manuscript.

Funding

This study was supported by grants from the Guangxi Medical and Health Appropriate Technology Development and Application Project (S2020062).

Data availability

The datasets used and analysed during the current study are available from the corresponding author upon reasonable request.

Declarations

Ethics approval and consent to participate

All experimental procedures were approved by the Ethics Committee of Guangxi Medical University (ethical batch number: No. 202407006) and were conducted in accordance with the National Institutes of Health Guide for the Care and Use of Animals.

Consent for publication

Not applicable.

Competing interests

The authors declare that they have no conflict of interests.

Author details

¹Department of Geriatric rehabilitation/Clinical Research Center for Geriatric Disorders of Guangxi Zhuang Autonomous Region, Jiangbin Hospital of Guangxi Zhuang Autonomous Region, No 85 Hedi Road, Nanning 530021, Guangxi Zhuang Autonomous Region, China

²Department of Neurology, Jiangbin Hospital of Guangxi Zhuang Autonomous Region, No 85 Hedi Road, Guangxi Zhuang Autonomous Region, Nanning 530021, China

Received: 23 October 2024 / Accepted: 12 April 2025

Published online: 28 May 2025

References

1. Boison D, Steinhäuser C. Epilepsy and astrocyte energy metabolism. *Glia*. 2018;66:1235–43.
2. Li S, Huang H, Wei X, et al. The recycling of AMPA Receptors/GABA_A receptors is related to neuronal excitation/inhibition imbalance and May be regulated by KIF5A. *Annals Translational Med*. 2022;10:1103–1103.
3. Betjemann JP, Lowenstein DH. Status epilepticus in adults. *Lancet Neurol*. 2015;14:615–24.
4. Li S, Wei X, Huang H, et al. Neuroplastin exerts antiepileptic effects through binding to the A1 subunit of GABA type A receptors to inhibit the internalization of the receptors. *J Translational Med*. 2023;21:707.
5. Zhao W, Li M, Li WS, Li Z, Li H. CircRNA SRRM4 affects glucose metabolism by regulating PKM alternative splicing via SRSF3 deubiquitination in epilepsy. *Neuropathol Appl Neurobiol*. 2023;49:e12850.
6. Dossi E, Rouach N. Pannexin 1 channels and ATP release in epilepsy: two sides of the same coin. *Purinergic Signalling*. 2021;17:533–48.
7. Angamo E, ul Haq R, Rösner J et al. Contribution of intrinsic lactate to maintenance of seizure activity in neocortical slices from patients with Temporal lobe epilepsy and in rat entorhinal cortex. *Int J Mol Sci* 2017;18.
8. Sada N, Lee S, Katsu T, Otsuki T, Inoue T. Epilepsy treatment. Targeting LDH enzymes with a stiripentol analog to treat epilepsy. *Science*. 2015;347:1362–7.
9. Hildebrand MS, Damiano JA, Mullen SA, et al. Glucose metabolism transporters and epilepsy: only GLUT1 has an established role. *Epilepsia*. 2014;55:e18–21.
10. Theodore WH, Kelley K, Toczek MT, Gaillard WD. Epilepsy duration, febrile seizures, and cerebral glucose metabolism. *Epilepsia*. 2004;45:276–9.
11. Scorza FA, de Almeida A-CG, Scorza CA, Finsterer J. Sudden unexpected death in epilepsy and abnormal glucose metabolism in the rat insular cortex: A brain within the heart. *Clinics* 2022;77.
12. Liu X, Nie L, Zhang Y, et al. Actin cytoskeleton vulnerability to disulfide stress mediates Disulfidptosis. *Nat Cell Biol*. 2023;25:404–14.
13. Liu X, Olszewski K, Zhang Y, et al. Cystine transporter regulation of Pentose phosphate pathway dependency and disulfide stress exposes a targetable metabolic vulnerability in cancer. *Nat Cell Biol*. 2020;22:476–86.
14. Joly JH, Delfarah A, Phung PS, Parrish S, Graham NA. A synthetic lethal drug combination mimics glucose deprivation-induced cancer cell death in the presence of glucose. *J Biol Chem*. 2020;295:1350–65.
15. Koppula P, Zhang Y, Shi J, Li W, Gan B. The glutamate/cystine antiporter SLC7A11/xCT enhances cancer cell dependency on glucose by exporting glutamate. *J Biol Chem*. 2017;292:14240–9.
16. Yao H-F, Ge J, Chen J, et al. CASC8 activates the pentose phosphate pathway to inhibit disulfidptosis in pancreatic ductal adenocarcinoma through the c-Myc-GLUT1 axis. *J Exp Clinical Cancer Res*. 2025;44:26.
17. Liu X, Zhuang L, Gan B. Disulfidptosis: disulfide stress-induced cell death. *Trends Cell Biol*. 2024;34:327–37.
18. Liu X, Zhang Y, Zhuang L, Olszewski K, Gan B. NADPH debt drives redox bankruptcy: SLC7A11/xCT-mediated cystine uptake as a double-edged sword in cellular redox regulation. *Genes Dis*. 2021;8:731–45.

19. Koppula P, Zhang Y, Zhuang L, Gan B. Amino acid transporter SLC7A11/xCT at the crossroads of regulating redox homeostasis and nutrient dependency of cancer. *Cancer Commun (Lond)*. 2018;38:12.
20. Brekke E, Berger HR, Widerøe M, Sonnewald U, Morken TS. Glucose and intermediary metabolism and Astrocyte–Neuron interactions following neonatal Hypoxia–Ischemia in rat. *Neurochem Res*. 2016;42:115–32.
21. Dai C, Tan C, Zhao L, et al. Glucose metabolism impairment in Parkinson's disease. *Brain Res Bull*. 2023;199:110672.
22. Wang Q, Duan L, Li X et al. Glucose metabolism, neural cell senescence and Alzheimer's disease. *Int J Mol Sci* 2022;23.
23. Ma S, Wang D, Xie D. Identification of disulfidptosis-related genes and subgroups in Alzheimer's disease. *Front Aging Neurosci* 2023;15.
24. Zhao S, Zhuang H, Ji W, Cheng C, Liu Y. Identification of Disulfidptosis-Related genes in ischemic stroke by combining Single-Cell sequencing, machine learning algorithms, and in vitro experiments. *Neuromol Med* 2024;26.
25. Schwächter EM, Velíšek. Velísková J. L. Correlation between extracellular glucose and seizure susceptibility in adult rats. *Ann Neurol*. 2003;53:91–101.
26. Du K, He M, Zhao D et al. Mechanism of cell death pathways in status epilepticus and related therapeutic agents. *Biomed Pharmacother* 2022;149.
27. Eva Brekke. Glucose and intermediary metabolism and Astrocyte–Neuron interactions following neonatal Hypoxia–Ischemia in rat. *Neurochem Res* 2017;42:115–32.
28. Shao H, Li. A new perspective on HIV: effects of HIV on brain-heart axis. *Front Cardiovasc Med*. 2023;10:1226782.
29. McClory. H, Williams D, Sapp E et al. Glucose transporter 3 is a rab11-dependent trafficking cargo and its transport to the cell surface is reduced in neurons of CAG140 Huntington's disease mice. *Acta Neuropathol Commun* 2014;2.
30. Li S, Zheng Y, Long Q et al. Drug–drug interactions between Propofol and ART drugs: inhibiting neuronal activity by affecting glucose metabolism. *CNS Neurosci Ther* 2023;30.
31. Sultana P, Novotny J. Rab11 and its role in neurodegenerative diseases. *ASN Neuro* 2022;14.
32. Moya-Alvarado G, Guerra MV, Tiburcio R, Bravo E, Bronfman FC. The Rab11-regulated endocytic pathway and BDNF/TrkB signaling: roles in plasticity changes and neurodegenerative diseases. *Neurobiol Dis* 2022;171.
33. Hamdan FF, Myers CT, Cossette P, et al. High rate of recurrent de Novo mutations in developmental and epileptic encephalopathies. *Am J Hum Genet*. 2017;101:664–85.
34. Fang Z, Sun Q, Yang H, Zheng J. SDHB suppresses the tumorigenesis and development of CcRCC by inhibiting Glycolysis. *Front Oncol* 2021;11.
35. Peng M, Yang D, Hou Y et al. Intracellular citrate accumulation by oxidized ATM-mediated metabolism reprogramming via PFKP and CS enhances hypoxic breast cancer cell invasion and metastasis. *Cell Death Dis* 2019;10.
36. Wang Q, Li S, Xu C et al. Glutaminolysis Inhibition boosts photodynamic therapy to eliminate cancer stem cells. *Biomaterials* 2024;306.
37. Chan K, Robert F, Oertlin C et al. eIF4A supports an oncogenic translation program in pancreatic ductal adenocarcinoma. *Nat Commun* 2019;10.
38. Hendrix RD, Ou Y, Davis JE, et al. Alzheimer amyloid-beta-peptide disrupts membrane localization of glucose transporter 1 in astrocytes: implications for glucose levels in brain and blood. *Neurobiol Aging*. 2021;97:73–88.
39. Shin B-C, Cepeda C, Eghbali M, Byun SY, Levine MS, Devaskar SU. Adult glut3 homozygous null mice survive to demonstrate neural excitability and altered neurobehavioral responses reminiscent of neurodevelopmental disorders. *Exp Neurol* 2021;338.
40. Li X, Valencia A, McClory H, Sapp E, Kegel KB, DiFiglia M. Deficient Rab11 activity underlies glucose hypometabolism in primary neurons of Huntington's disease mice. *Biochem Biophys Res Commun*. 2012;421:727–30.
41. Trinka E, Cock H, Hesdorffer D, et al. A definition and classification of status epilepticus– Report of The ILAE Task force on classification of status epilepticus. *Epilepsia*. 2015;56:1515–23.
42. Zhang S, Lachance BB, Mattson MP, Jia X. Glucose metabolic crosstalk and regulation in brain function and diseases. *Prog Neurobiol* 2021;204.
43. Peng W, Liu X, Tan C, et al. Zinc- α 2-glycoprotein relieved seizure-induced neuronal glucose uptake impairment via insulin-like growth factor 1 receptor-regulated glucose transporter 3 expression. *J Neurochem*. 2020;157:695–709.
44. Osés JP, Muller AP, Strogulski NR, et al. Sustained elevation of cerebrospinal fluid glucose and lactate after a single seizure does not parallel with mitochondria energy production. *Epilepsy Res*. 2019;152:35–41.
45. Qu. EH, Unsgård. H, Sletvold. G, O HH. Sonnewald. U. Effects of Pentyleneetetrazole and glutamate on metabolism of [U-(13)C]glucose in cultured cerebellar granule neurons. *Neurochem Int*. 2002;40:181–7.
46. Neurons and microvessels express the brain glucose transporter protein GLUT3. *ZD. Proc Natl Acad Sci U S A*. 1992;89:733–7.
47. Dwyer DS. Model of the 3-D structure of the GLUT3 glucose transporter and molecular dynamics simulation of glucose transport. *Proteins*. 2001;42:531–41.
48. An Y, Varma VR, Varma S, et al. Evidence for brain glucose dysregulation in Alzheimer's disease. *Alzheimer's Dement*. 2017;14:318–29.
49. Liu J, Zhang J-P, Shi M, et al. Rab11a and HSP90 regulate recycling of extracellular α -Synuclein. *J Neurosci*. 2009;29:1480–5.
50. Nishino H, Saito T, Wei R, et al. The LMTK1-TBC1D9B-Rab11A cascade regulates dendritic spine formation via endosome trafficking. *J Neurosci*. 2019;39:9491–502.
51. Janusz-Kaminska A, Brzozowska A, Tempes A et al. Rab11 regulates autophagy at dendritic spines in an mTOR- and NMDA-dependent manner. *Mol Biol Cell* 2024;35.
52. Nisa A, Kipper FC, Panigrahy D, Tiwari S, Kupz A, Subbian S. Different modalities of host cell death and their impact on Mycobacterium tuberculosis infection. *Am J Physiol Cell Physiol*. 2022;323:C1444–74.
53. Fricker M, Tolkovsky AM, Borutaite V, Coleman M, Brown GC. Neuronal Cell Death Physiological Reviews. 2018;98:813–80.
54. Li M, Wang Z-W, Fang L-J, Cheng S-Q, Wang X, Liu N-F. Programmed cell death in atherosclerosis and vascular calcification. *Cell Death Dis* 2022;13.
55. Cobine PA, Brady DC, Cuproptosis. Cellular and molecular mechanisms underlying copper-induced cell death. *Mol Cell*. 2022;82:1786–7.
56. Berger I, Hershkovitz E, Shaag A, Edvardson S, Saada A, Elpeleg O. Mitochondrial complex I deficiency caused by a deleterious NDUFA11 mutation. *Ann Neurol*. 2008;63:405–8.
57. Abrosimov R, Baeken MW, Hauf S, et al. Mitochondrial complex I Inhibition triggers NAD⁺-independent glucose oxidation via successive NADPH formation, futile fatty acid cycling, and FADH2 oxidation. *GeroScience*. 2024;46:3635–58.
58. Frambach SJCM, de Haas R, Smeitink JAM, Russel FGM, Schirris TJJ. Restoring cellular NAD(P)H levels by PPAR α and LXR α stimulation to improve mitochondrial complex I deficiency. *Life Sci* 2022;300.
59. Gombodorj N, Azuma Y, Yokobori T, et al. RAB11A expression is associated with Cancer aggressiveness through regulation of FGFR-Signaling in lung squamous cell carcinoma. *Ann Surg Oncol*. 2022;29:7149–62.
60. Li X, Valencia A, Sapp E, et al. Aberrant Rab11-Dependent trafficking of the neuronal glutamate transporter EAAC1 causes oxidative stress and cell death in Huntington's disease. *J Neurosci*. 2010;30:4552–61.
61. Xiang T, Luo X, Zeng C, Li S, Ma M, Wu Y. Klotho ameliorated cognitive deficits in a Temporal lobe epilepsy rat model by inhibiting ferroptosis. *Brain Res* 2021;1772.
62. Sokolova TV, Zabrodskaya YM, Litovchenko AV et al. Relationship between neuroglial apoptosis and neuroinflammation in the epileptic focus of the brain and in the blood of patients with Drug-Resistant epilepsy. *Int J Mol Sci* 2022;23.
63. Peng Z, Zhang C, Yan L et al. EPA is more effective than DHA to improve depression-Like behavior, glia cell dysfunction and Hippocampal apoptosis signaling in a chronic Stress-Induced rat model of depression. *Int J Mol Sci* 2020;21.
64. Murase S. A new model for developmental neuronal death and excitatory/inhibitory balance in hippocampus. *Mol Neurobiol*. 2014;49:316–25.
65. Wu Z, Deshpande T, Henning L, Bedner P, Seifert G, Steinhäuser C. Cell death of hippocampal CA1 astrocytes during early epileptogenesis. *Epilepsia*. 2021;62:1569–83.
66. Engel T, Plesnila N, Pehn JHM, Henshall DC. In vivo contributions of BH3-Only proteins to neuronal death following seizures, ischemia, and traumatic brain injury. *J Cereb Blood Flow Metabolism*. 2011;31:1196–210.
67. Wang J, Chen Y, Wang Q, van Luitelaar G, Sun M. The effects of lamotrigine and Ethosuximide on seizure frequency, neuronal loss, and astrogliosis in a model of temporal-lobe epilepsy. *Brain Res*. 2019;1712:1–6.
68. Yu L, Yang J, Yu W, Cao J, Li X. Rhein attenuates PTZ-induced epilepsy and exerts neuroprotective activity via Inhibition of the TLR4-NF κ B signaling pathway. *Neurosci Lett* 2021;758.

Publisher's note

Springer Nature remains neutral with regard to jurisdictional claims in published maps and institutional affiliations.